



Contents lists available at ScienceDirect

Spectrochimica Acta Part A: Molecular and Biomolecular Spectroscopy

journal homepage: www.elsevier.com/locate/saa

Synthesis, spectral and third-order nonlinear optical properties of terpyridine Zn(II) complexes based on carbazole derivative with polyether group



Ming Kong^a, Yanqiu Liu^a, Hui Wang^a, Junshan Luo^a, Dandan Li^a, Shengyi Zhang^a, Shengli Li^a, Jieying Wu^{a,*}, Yupeng Tian^{a,b,*}

^a Department of Chemistry, Key Laboratory of Functional Inorganic Material Chemistry of Anhui Province, Anhui University, Hefei 230039, PR China

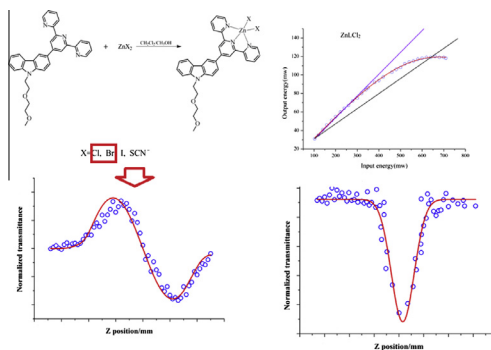
^b State Key Laboratory of Coordination Chemistry, Nanjing University, Nanjing 210093, PR China

HIGHLIGHTS

- Four Zn(II) terpyridine complexes with different coordination anions were designed and synthesized.
- The linear and nonlinear spectroscopic properties were carried out.
- The results revealed that two Zn(II) complexes possessed larger TPA cross-sections.
- The complex of ZnLCl₂ showed superior optical power limiting property.

GRAPHICAL ABSTRACT

Four novel Zn(II) terpyridine complexes (ZnLCl₂, ZnLBr₂, ZnLI₂, ZnL(SCN)₂) based on carbazole derivative group were designed, synthesized and fully characterized. Their photophysical properties including absorption and one-photon excited fluorescence, two-photon absorption (TPA) and optical power limiting (OPL) were further investigated systematically and interpreted on the basis of theoretical calculations (TD-DFT). The results of NLO determination revealed that two Zn(II) complexes possessed larger two-photon absorption cross-sections and ZnLCl₂ complex showed superior optical power limiting property which suggested a large polarizability, meeting the requirements for third-order NLO materials offering promise for applications in optical limiting in the near infrared region.



ARTICLE INFO

Article history:

Received 27 March 2014
Received in revised form 8 July 2014
Accepted 18 July 2014
Available online 27 July 2014

Keywords:

Terpyridine
Carbazole derivative

ABSTRACT

Four novel Zn(II) terpyridine complexes (ZnLCl₂, ZnLBr₂, ZnLI₂, ZnL(SCN)₂) based on carbazole derivative group were designed, synthesized and fully characterized. Their photophysical properties including absorption and one-photon excited fluorescence, two-photon absorption (TPA) and optical power limiting (OPL) were further investigated systematically and interpreted on the basis of theoretical calculations (TD-DFT). The influences of different solvents on the absorption and One-Photon Excited Fluorescence (OPEF) spectral behavior, quantum yields and the lifetime of the chromophores have been investigated in detail. The third-order nonlinear optical (NLO) properties were investigated by open/closed aperture Z-scan measurements using femtosecond pulse laser in the range from 680 to 1080 nm. These results

* Corresponding authors. Address: Department of Chemistry, Key Laboratory of Functional Inorganic Material Chemistry of Anhui Province, Anhui University, Hefei 230039, PR China (Y.p. Tian).

E-mail addresses: jywu1957@163.com (J. Wu), yptian@ahu.edu.cn (Y.p. Tian).

Photophysical properties
TD-DFT calculation
Third-order nonlinear optical (NLO)
Optical power limiting

revealed that ZnLCl₂ and ZnLBr₂ exhibited strong two-photon absorption and ZnLCl₂ showed superior optical power limiting property.

© 2014 Elsevier B.V. All rights reserved.

Introduction

Among so many *N*-heteroatom ligands, analogous 2, 2':6', 2''-terpyridine compounds as a electron acceptor (A) have been attracted considerable attention in diverse areas of current research [1–7]. This kinds of terpyridine in constructing specific, stable metal complexes and self-assembly with unique properties have evolved from a fundamental scientific field into daily-life applications such as biological medicine [8,9], nanotechnology [10,11], catalysis [12–18], polymer science [19–21], optical materials which have led to applications in solar cells, probe, self-assembly, biopolymer, and for the localized release of bio-active species [22–34]. Such these special optical materials exhibiting strong third-order nonlinear optical (NLO) absorptions have attracted considerable interests because of their potential applications in optical switching, three-dimensional (3D) fluorescence imaging, 3D optical data storage, 3D lithographic microfabrication and optical power limiting [35–40].

Zinc (d¹⁰) possessed a great diversity of properties and can easily combine with terpyridine ligand [41–43]. As a result, four Zn(II) terpyridine complexes with different coordination anions were designed and synthesized to study how different kinds of anions carry out an influence on their spectroscopic properties. Within the ligand molecule, 9-(2-(2-methoxyethoxy) ethyl)-9H-carbazole group was introduced as a electron donor (D) and efficient π -electron bridge, polyether chain attached to the carbazole group was to increase the solubility of these D–A type ligand (coordination compounds). So this design strategy combined those advantages to construct novel model terpyridine compounds. Herein, the synthesis and their photophysical properties of them with different coordination anions were systematically investigated experimentally. In addition, time-dependent density functional theory (DFT) calculations were also performed to offer a suggestion for the relationships between the structures and properties.

Experimental section

General methods

All chemicals were commercially available and used as obtained. The solvents were purified by conventional methods before use. The ¹H NMR and ¹³C NMR spectra recorded on at 25 °C using Bruker Avance 400 spectrometer were reported as parts per million (ppm) from TMS. IR spectra were recorded on NEXUS 870 (Nicolet) spectrophotometer in the 400–4000 cm⁻¹ region using a powder sample on a KBr plate. Elemental analyses were performed with a Perkin Elmer 240C elemental analyzer. Mass spectra were obtained on a Micromass MALDI-TOF-MS.

Absorption spectra were obtained on a UV-265 spectrophotometer, Fluorescence measurements were performed using a Hitachi F-7000 fluorescence spectrophotometer excited at the longest absorption band. The concentration of sample solution was 1.0 × 10⁻⁵ mol/L. For time-resolved fluorescence measurements, the fluorescence signals were collimated and focused onto the entrance slit of a monochromator with the output plane equipped with a photomultiplier tube (HORIBA HuoroMax-4P). The decays were analyzed by 'least-squares'. The quality of the exponential fits was evaluated by the goodness of fit (χ^2).

To better identify the charge transition, time-dependent density functional theory (TD-DFT) calculations were carried out in vacuo. Geometry optimizations were carried out with B3LYP functional without any symmetry restraint, and the TD-DFT calculations were performed on the optimized structure with B3LYP functional. All calculations, including optimizations and TD-DFT, were performed with the G03 software. Geometry optimization of the singlet ground state and the TD-DFT calculation of the lowest 50 singlet–singlet excitation energies were calculated with a basis set composed of 6-31 G for C H N O atoms and the Lanl2dz basis set for Cl, Br, I, Zn atoms. An analytical frequency confirmed evidence that the calculated species represents a true minimum without imaginary frequencies on the respective potential energy surface. The lowest 40 spin-allowed singlet–singlet transitions, up to energy of about 5 eV, were taken into account in the calculation of the absorption spectra.

NLO properties were measured by the Z-scan technique with a femtosecond laser pulse and Ti: 95 sapphire system (680–1080 nm, 80 MHz, 140 fs, Chameleon II) as the light source. The beam was spatially filtered to remove higher-order modes and tightly focused using a 5 cm focal length lens. The incident average power of 400 mW was adjusted by a Glan prism. The thermal heating of the sample with high repetition rate laser pulse was removed by the use of a mechanical chopper running at 10 Hz. A 1 mm cell of the sample in DMF at 1.0 × 10⁻³ mol L⁻¹ was put in the light path, and all measurements were carried out at room temperature.

Synthesis

Preparation of 9-(2-(2-methoxyethoxy) ethyl)-9H-carbazole-3-carbaldehyde (**m3**)

m1 Tetrabutylammonium (1.37 g, 4.25 mmol) and 2-(2-(2-methoxyethoxy)ethoxy) ethanol dissolved in 150 mL CH₂Cl₂ were added into 500 mL round-bottom flask and stirred at room temperature for 1 h while 120 mL 30% NaOH was poured into it. 4-Methylbenzene-1-sulfonyl chloride (30.50 g, 160 mmol) dissolved in 150 mL CH₂Cl₂ was added dropwise. After the reaction mixture was stirred at room temperature for 24 h, the mixture was poured into water and the liquid was collected. The oily liquid was dried by anhydrous magnesium sulfate. Colorless oily liquid **m1** was got with yield 89.2%.

m2 NaH (4.80 g, 200 mmol) with DMF 25 mL were added together into round-bottom flask, then 9H-carbazole (16.70 g, 100 mmol) dissolved in DMF was added dropwise using dropping funnel isolating atmosphere. After 2 h **m1** (30.10 g, 110 mmol) was added and stirred at 65 °C for 15 h. The mixture was poured into plenty of water and its pH was adjusted to about 6 using diluted hydrochloric acid. Ethyl acetate was used to extract the mixture and dried by anhydrous magnesium sulfate. The residue was chromatographed over silica gel. Yellow oily liquid **m2** was obtained with yield 82%.

m3 DMF (4.44 g, 60 mmol) was added in 250 mL round-bottom flask and POCl₃ (10.00 g, 65 mmol) was added dropwise using dropping funnel slowly. After white solid was successfully generated, **m2** (13.50 g, 50 mmol) dissolved in chloroform was added. When the solid mixture was thawed out, it was stirred at 65 °C for 18 h. The mixture was poured into large amounts of water and its pH was adjusted to about 8.0 using NaOH aqueous solution. Anhydrous magnesium sulfate was used for drying the mixture

after extracting the mixture by CH_2Cl_2 . The residue was chromatographed over silica gel using ethyl acetate–petroleum ether (volume ratio is 1:5). White solid **m3** was obtained with yield 63%. ^1H NMR (CD_3COCD_3 , 400 MHz) δ (ppm) = 3.14 (s, 3H), 3.33–3.34 (q, 2H), 3.49–3.50 (q, 2H), 3.91–3.94 (t, 2H), 4.64–4.66 (t, 2H), 7.30–7.33 (t, 1H), 7.52–7.55 (t, 1H), 7.68–7.70 (d, 1H), 7.75–7.77 (d, 1H), 7.99–8.01 (d, 1H), 8.26–8.28 (d, 1H), 8.69 (s, 1H), 10.10 (s, 1H).

Preparation of 3-([2,2':6',2''-terpyridin]-4'-yl)-9-(2-(2-methoxyethoxy) ethyl)-9H-carbazole (L)

m4 Pyridine (216 mL) and I_2 (37.60 g, 150 mmol) was added in 500 mL round-bottom flask. The mixture was heated to 65 °C stirring until they were dissolved. 1-(Pyridin-2-yl) ethanone (21.60 g, 178 mmol) was added in above mixture and heated to 95 °C for 3 h. And then, the reaction mixture was allowed to cool to room temperature and the solid was collected on a fritted filter funnel. The crude product was subsequently washed with CH_2Cl_2 . The black solid **m4** was obtained with yield 64%.

m5 m3 (8.91 g, 30 mmol) Dissolved in ethyl alcohol (200 mL) was added into 500 mL round-bottom flask. Subsequently 1-(pyridin-2-yl) ethanone (3.63 g, 30 mmol) and NaOH (2.80 g, 70 mmol) were added into it under stirring. After 15 h, orange solid **m5** was collected with fritted filter funnel and washed with water.

L m5 (2.00 g, 5 mmol) and **m4** (1.63 g, 5 mmol) were dissolved in 50 mL methyl alcohol. After stirring for 20 min, NH_4Ac (2.31 g, 30 mmol) was added. The mixture was refluxed for 24 h. The crude product was collected with fritted filter funnel and washed with water. The mixture was drying with anhydrous magnesium sulfate and chromatographed over silica gel using CH_2Cl_2 – CH_3OH (volume ratio is 10:1), giving brown solid **L** (0.77 g) with yield 31%. ^1H NMR (CD_3COCD_3 , 400 MHz) δ (ppm) = 3.18 (s, 3H), 3.36–3.39 (q, 2H), 3.52–3.54 (q, 2H), 3.93–3.96 (t, 2H), 4.63–4.66 (t, 2H), 7.26–7.30 (t, 1H), 7.47–7.53 (q, 3H), 7.66–7.68 (d, 1H), 7.81–7.83 (d, 1H), 7.99–8.06 (q, 3H), 8.36–8.37 (d, 1H), 8.76–8.77 (d, 5H), 8.95 (s, 2H) (Fig. S1). ^{13}C NMR (CDCl_3 , 100 MHz): δ (ppm) = 155.47, 155.23, 150.38, 149.24, 140.99, 140.80, 137.33, 128.26, 126.09, 124.54, 124.35, 122.95, 122.27, 120.92, 120.78, 119.27, 118.79, 117.88, 110.39, 109.81, 71.23, 70.50, 69.78, 68.80, 58.02, 43.06. IR (KBr, cm^{-1}): 3435 (m), 3049 (vw), 2908 (w), 1583 (s), 1466 (s), 1126 (m), 788 (m), 750 (m). m.p. 97 °C. MALDI-TOF-MS: m/z , cal.: 500.2, found: 501.23 (Fig. S2).

Preparation of Zn (II) complexes

ZnLI₂: **L** (0.5 g, 1 mmol) dissolved in 20 mL CH_2Cl_2 and ZnI_2 (0.32 g, 1 mmol) dissolved in 4 mL methyl alcohol were added in 50 mL round-bottom flask then heated to refluxing. After the reaction, the liquid was cooled to room temperature and the solid was extracted by fritted filter funnel giving yellow solid **ZnLI₂** (0.68 g) after washed several times with water and ethyl alcohol with yield 85%. ^1H NMR (CD_3SOCD_3 , 400 MHz) δ (ppm) = 3.14 (s, 3H), 3.49–3.53 (q, 2H), 3.89–3.92 (t, 2H), 4.72–4.74 (t, 2H), 7.37–7.40 (t, 1H), 7.57–7.60 (t, 1H), 7.78–7.80 (d, 1H), 8.00–8.01 (d, 3H), 8.62–8.64 (d, 1H), 8.94 (s, 1H), 9.17–9.27 (m, 4H), 9.36 (s, 1H), 9.52 (s, 1H). ^{13}C NMR (CD_3SOCD_3 , 100 MHz) δ (ppm) = 155.62, 155.55, 150.50, 149.22, 141.08, 140.91, 137.30, 128.35, 126.29, 124.61, 124.55, 123.05, 122.43, 120.96, 120.65, 119.36, 118.16, 117.40, 110.92, 109.34, 71.34, 70.06, 69.46, 68.85, 58.15, 43.07. IR (KBr, cm^{-1}): 3443 (m), 3049 (vw), 2925 (w), 1593 (s), 1472 (s), 1102 (m), 790 (m), 748 (m). Anal. Cal. for $\text{C}_{32}\text{H}_{28}\text{I}_2\text{N}_4\text{O}_2\text{Zn}$: C, 46.88; H, 3.44; N, 6.83; found: C, 46.78; H, 3.394; N, 6.81. m.p. 325 °C. MALDI-TOF-MS: cal.: 819.78, found: 690.59 ([M-I-2H]⁺) (Fig. S6).

Other three complexes were prepared by a similar procedure with that of **ZnLI₂** just with ZnI_2 replaced by ZnCl_2 , ZnBr_2 , and $\text{Zn}(\text{SCN})_2$.

ZnLCl₂: ^1H NMR (CD_3SOCD_3 , 400 MHz) δ (ppm) = 3.19 (s, 3H), 3.56–3.58 (q, 2H), 3.90–3.93 (t, 2H), 4.64–4.66 (t, 2H), 7.32–7.36 (t, 1H), 7.54–7.56 (t, 1H), 7.62–7.64 (t, 1H), 7.72–7.76 (t, 1H), 8.05–8.09 (t, 1H), 8.31–8.35 (t, 1H), 8.68–8.78 (q, 4H), 8.91 (s, 2H), 9.04 (s, 1H) (Fig. S3). ^{13}C NMR (CD_3SOCD_3 , 100 MHz) δ (ppm) = 156.47, 154.57, 152.30, 147.33, 140.78, 140.10, 137.01, 128.26, 127.88, 126.90, 125.70, 122.23, 121.27, 120.32, 120.88, 119.74, 118.76, 117.28, 110.35, 109.81, 71.34, 69.76, 68.85, 58.15, 43.07. IR (KBr, cm^{-1}): 3441 (m), 3062 (vw), 2925 (w), 1594 (s), 1472 (s), 1118 (m), 791 (m), 748 (m). Anal. Cal. for $\text{C}_{32}\text{H}_{28}\text{Cl}_2\text{N}_4\text{O}_2\text{Zn}$: C, 60.35; H, 4.43; N, 8.80; found: C, 60.31; H, 4.40; N, 8.74. m.p. 295 °C. MALDI-TOF-MS: cal.: 636.88, found: 598.48 ([M-Cl-3H]⁺) (Fig. 1).

ZnLBr₂: ^1H NMR (CD_3SOCD_3 , 400 MHz) δ (ppm) = 3.16 (s, 3H), 3.52–3.55 (q, 2H), 3.89–3.91 (t, 2H), 4.68–4.70 (t, 2H), 7.34–7.38 (t, 1H), 7.55–7.58 (t, 1H), 7.74–7.77 (d, 1H), 7.87–7.88 (d, 3H), 8.31–8.45 (m, 4H), 8.90–8.98 (q, 4H), 9.16 (s, 3H). ^{13}C NMR (CD_3SOCD_3 , 100 MHz) δ (ppm) = 155.85, 155.17, 150.80, 149.90, 140.78, 140.47, 137.53, 128.49, 126.90, 124.62, 124.42, 123.25, 122.23, 120.95, 120.65, 119.36, 118.46, 117.86, 110.32, 109.87, 71.34, 70.57, 69.76, 68.85, 58.15, 43.07. IR (KBr, cm^{-1}): 3443 (m), 3054 (vw), 2925 (w), 1593 (s), 1472 (s), 1101 (m), 790 (m), 747 (m). Anal. Cal. for $\text{C}_{32}\text{H}_{28}\text{Br}_2\text{N}_4\text{O}_2\text{Zn}$: C, 52.96; H, 3.89; N, 7.72; found: C, 52.91; H, 3.87; N, 7.69. m.p. 300 °C. MALDI-TOF-MS: cal.: 725.78, found: 644.5 ([M-Br-H]⁺) (Fig. S5).

ZnL(SCN)₂: ^1H NMR (CD_3SOCD_3 , 400 MHz) δ (ppm) = 3.13 (s, 3H), 3.49–3.51 (t, 2H), 3.86–3.88 (t, 2H), 4.66–4.68 (t, 2H), 7.33–7.35 (t, 1H), 7.53–7.55 (t, 1H), 7.72–7.74 (d, 1H), 7.88–7.90 (d, 3H), 8.40–8.42 (q, 4H), 8.83 (s, 1H), 9.04–9.17 (m, 4H), 9.52 (s, 1H). ^{13}C NMR (CD_3SOCD_3 , 100 MHz) δ (ppm) = 156.37, 156.16, 150.50, 149.24, 141.11, 140.99, 137.19, 128.67, 127.38, 124.77, 124.56, 122.95, 122.96, 121.23, 120.76, 119.47, 118.89, 117.93, 110.57, 110.26, 71.32, 70.94, 69.72, 68.73, 58.31, 43.10. IR (KBr, cm^{-1}): 3443 (m), 3062 (vw), 2920 (w), 2072 (vs), 1591 (s), 1472 (s), 1101 (m), 789 (m), 747 (m) (Fig. S4). Anal. Cal. for $\text{C}_{34}\text{H}_{28}\text{S}_2\text{N}_6\text{O}_2\text{Zn}$: C, 59.86; H, 4.14; N, 12.32; found: C, 59.87; H, 4.107; N, 12.26. m.p. 321 °C. MALDI-TOF-MS: cal.: 682.14, found: 621.44 ([M-S-C-N-3H]⁺) (Fig. S7).

Results and discussion

Synthesis and characteristic discussion

Four new Zn(II) terpyridine complexes (ZnLCl_2 , ZnLBr_2 , ZnLI_2 , $\text{ZnL}(\text{SCN})_2$) based on carbazole derivative group were synthesized by efficient synthetic routes and the processes were depicted in Scheme 1 (seeing supporting information). Those target products have been characterized by IR, ^1H NMR, ^{13}C NMR, elemental analyses and MALDI-TOF-MS. From the infrared spectrum of $\text{ZnL}(\text{SCN})_2$, a new peak at 2071.89 cm^{-1} can be observed, which was contributed to the characteristic peak of SCN (Fig. S4). By contrasting the ^1H NMR spectra of **L** with ZnLCl_2 or the other complexes, the chemical shifts of H located in the coordinated pyridine ring shifted to low field because of the electron density of H decreasing (Figs. S1 and S3). Comparing the MALDI-TOF-MS of four complexes, the ZnLBr_2 was different from others and another peak which was composed of polymeric fragment was found (Fig. S5). Only one intense peak were found for the mass spectra of ZnLCl_2 , ZnLI_2 , ZnLSCN_2 , and **L** (Fig. 1). All the characterizations indicated that the ligand and its metal complexes were successfully obtained.

Linear absorption and TD-DFT studies

Table 1 summarized the photophysical data of all the compounds in different solvents. Clearly, two intense absorption bands

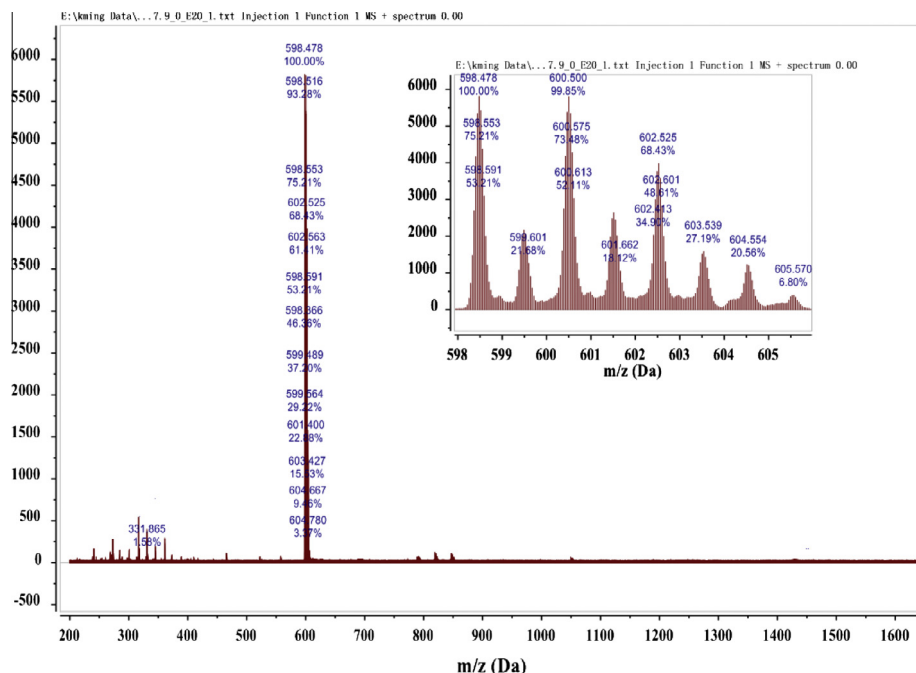


Fig. 1. MALDI-TOF-MS of ZnLCl_2 .

of **L** in the range of 290–330 nm ($\epsilon > 10^4$) showed hardly any shifts with increasing polarity of the solvents (Fig. 2). Three intense absorption bands of the four Zn(II) terpyridine complexes were observed, but showing weak solvatochromism, except ethyl alcohol solvent, indicating the complex molecules with fairly little difference in dipoles between ground and excited state (ZnLCl_2 as an example in Fig. 3). However, the two bands of complexes in the higher energy region are different from **L**. Compared with **L**, the absorption of 310–320 nm experienced a bathochromic shift on account of the formation of coordination bands which strengthens the capability of electron delocalization resulting in the energy gap decreasing between HOMO and LUMO. Also, a new emerging absorption band was observed in the lowest energy band about 370–395 nm showing weak solvatochromism. The maximum absorption band in the highest energy region about 280–290 nm causes an obvious blue shift contrasting with **L** (Fig. 4).

Table 2 exhibits the selected experimental and calculated optical data for the ligand and their Zn(II) complexes including energies and compositions of frontier orbital. The absorption spectra of the investigated compounds showing similar features were significantly confirmed by the means of theoretical calculation. Two intense absorption bands of **L** in the range of 290–330 nm ($\epsilon > 10^4$) which originating from $\text{HOMO(H)}-2 \rightarrow \text{LUMO(L)}+1$ and $\text{H} \rightarrow \text{L}+1$ were assigned to $\pi \rightarrow \pi^*$ transitions of terpyridine and $\pi \rightarrow \pi^*$ from carbazole to terpyridine were observed. The three absorption bands of four Zn(II) complexes were demonstrated to $\pi(\text{carbazole}) \rightarrow \pi(\text{terpyridine})^*$, $\pi \rightarrow \pi^*/\text{ICT}(\text{terpyridine} \rightarrow \text{terpyridine})$ and $\text{ICT}/\pi \rightarrow \pi(\text{carbazole} \rightarrow \text{terpyridine})$ from high energy to low energy regions which coming from identical transition and performing approximate transition energy attributing. The molecular orbital energy diagrams of the ligands and complexes were expressed in Fig. S10. Overall, the absorption spectral features were reasonably explained through the initial TD-DFT calculations.

One-Photon Excited Fluorescence (OPEF)

The one-photon fluorescence spectral data were listed in Table 1 including fluorescence quantum yields and lifetimes.

The influence of solvents on the fluorescence spectra was observed. The fluorescence intensity of **L** was strongest than those of the complexes. Clearly, the fluorescence (SPEF) spectra of **L** and the four complexes displayed a remarkable red-shifting and showed fluorescence quenching with increasing polarity of the solvent, especially for ZnLi_2 (Fig. S8). For example, in the spectrum of **L** in ethyl alcohol solvent, excited at 320 nm, a novel band with weak intensity was observed at 445 nm. The Stokes shifting reached a maximum of 8778 cm^{-1} . One interpretation could be given that the excited state energy was lower than ground state with increasing polarity of the solvents because of a larger enhanced dipole moment, and the energy gap between ground state and excited state declines, which explains the sensitivity of the emission spectra of these dipolar compounds to solvent polarity [44]. Besides, the ethyl alcohol solvent could generate intermolecular hydrogen bond with **L** resulting in an enhanced non-radioactive transition [45,46]. As a response, the photoluminescence (PL) quantum yields (ϕ) of **L** were lowered at the lowest level of 0.10 and a similarly with that of ZnLCl_2 and ZnLBr_2 . Furthermore, fluorescence lifetime of the complexes also prolonged which suggested that the molecule polarity of excited state must be larger than that of ground state enhancing dipole–dipole interactions. Interestingly, the fluorescence spectra of four complexes show weak bathochromic shift in the same solvent by the change of coordination anion from Cl^- to I^- , while show obvious bathochromic shifts comparing with **L** (Fig. 4). However, the fluorescence intensity of ZnLi_2 was obvious quenched accompanying low fluorescence quantum yields comparing the other three complexes (Fig. S8). This phenomenon was caused by heavy atom effect of I which enhances spin–orbital coupling and increases intersystem crossing rate from excited singlet state (S_1) to excited triplet state (T_1). Similarly, quenched effect of the fluorescence spectra in benzene solvents was because of the low solubility caused by the coordination band which enhanced the molecule polarity and declined the soluble possibility in weak polarity solvent. The fluorescence spectra of $\text{ZnI}(\text{SCN})_2$ show the most intensity contrasting other complexes. It was because of the molecule unit containing highly delocalized conjugated system formed by coordination anion of SCN^- (Fig. S9).

Table 1
Single-photon-related photophysical properties of L, ZnLCl₂, ZnLBr₂, ZnLI₂ and ZnL(SCN)₂ in several different solvents.

Compounds	Solvents	λ_{\max}^a (ϵ_{\max}^b)	λ_{\max}^c	$\Delta\nu^d$	Φ^e	τ^f	$10^{-9}k_r$ (s ⁻¹)	$10^{-9}k_{nr}$ (s ⁻¹)
L	Benzene	295(3.96),323(1.73)	388	5187	0.30	2.56	11.7	27.3
	Dichloromethane	294(4.39),321(1.91)	410	6762	0.27	2.76	9.8	26.4
	Ethyl acetate	293(4.24),320(1.88)	401	6312	0.24	2.55	9.4	29.8
	Ethyl alcohol	294(4.36),320(1.92)	445	8778	0.10	–	–	–
	Acetonitrile	292(4.37),321(1.90)	425	7623	0.22	–	–	–
	DMF	295(4.09),320(1.77)	430	7994	0.30	4.57	6.6	15.3
ZnLCl ₂	Benzene	286(2.79),310(2.12),369(1.31)	446	4679	0.23	2.65	8.68	29.1
	Dichloromethane	282(4.16),314(2.95),377(2.11)	491	6159	0.12	4.80	2.50	18.3
	Ethyl acetate	281(4.00),307(2.91),368(2.00)	474	6077	0.20	3.82	5.24	20.9
	Ethyl alcohol	282(4.29),316(2.58),390(1.88)	524	6557	0.06	3.00	2.00	31.3
	Acetonitrile	281(4.67),308(3.14),375(2.15)	523	7546	0.09	3.73	2.41	24.4
	DMF	286(4.92),317(2.72),382(0.83)	–	–	–	–	–	–
ZnLBr ₂	Benzene	288(3.06),313(2.38),372(1.57)	447	4510	0.10	2.52	3.97	35.7
	Dichloromethane	283(4.14),314(2.98),382(2.23)	490	5770	0.23	3.46	6.65	22.2
	Ethyl acetate	282(3.92),312(2.95),370(2.07)	474	5930	0.19	3.04	0.63	26.6
	Ethyl alcohol	283(4.35),316(2.62),390(1.98)	522	6483	0.04	2.99	1.34	32.1
	Acetonitrile	281(4.45),312(3.11),377(2.36)	524	7441	0.06	3.74	1.60	25.1
	DMF	286(4.72),317(2.65),382(0.90)	–	–	–	–	–	–
ZnLI ₂	Benzene	286(4.41),315(3.25),374(2.21)	440	4011	0.01	2.52	0.40	39.3
	Dichloromethane	283(4.97),313(3.42),380(2.60)	490	5908	0.10	4.06	2.46	22.2
	Ethyl acetate	281(4.89),308(3.49),373(2.57)	476	5801	0.02	4.00	0.50	24.5
	Ethyl alcohol	283(4.18),316(2.50),393(1.90)	521	6251	0.06	2.99	2.01	31.4
	Acetonitrile	281(4.82),312(3.11),382(2.37)	527	7203	0.03	3.71	0.81	26.2
	DMF	291(5.39),319(2.70),383(0.52)	–	–	–	–	–	–
ZnL(SCN) ₂	Benzene	290(3.10),312(2.47),395(1.82)	502	5396	0.01	1.94	0.52	51.0
	Dichloromethane	282(5.59),317(3.67),387(2.71)	499	5800	0.10	4.92	2.03	18.3
	Ethyl acetate	281(5.11),313(3.47),380(2.53)	496	6154	0.02	4.97	0.40	19.7
	Ethyl alcohol	282(3.87),314(2.33),388(1.67)	521	6579	0.06	3.00	2.00	31.3
	Acetonitrile	281(4.82),312(3.16),382(2.41)	524	7094	0.03	3.71	0.81	26.2
	DMF	287(5.34),321(2.97),380(1.11)	–	–	–	–	–	–

k_r , Calculated fluorescence emission rate, k_{nr} , calculated non-radiative transition rate.

^a Peak position of the longest absorption band.

^b Maximum molar absorbance in $10^4 \text{ mol}^{-1} \text{ L cm}^{-1}$.

^c Peak position of SPEF, excited at the maximum wavelength of absorption.

^d Stokes shift in cm^{-1} .

^e Quantum yields determined by using quinine sulfate as standard.

^f The fitted fluorescence lifetime (ns).

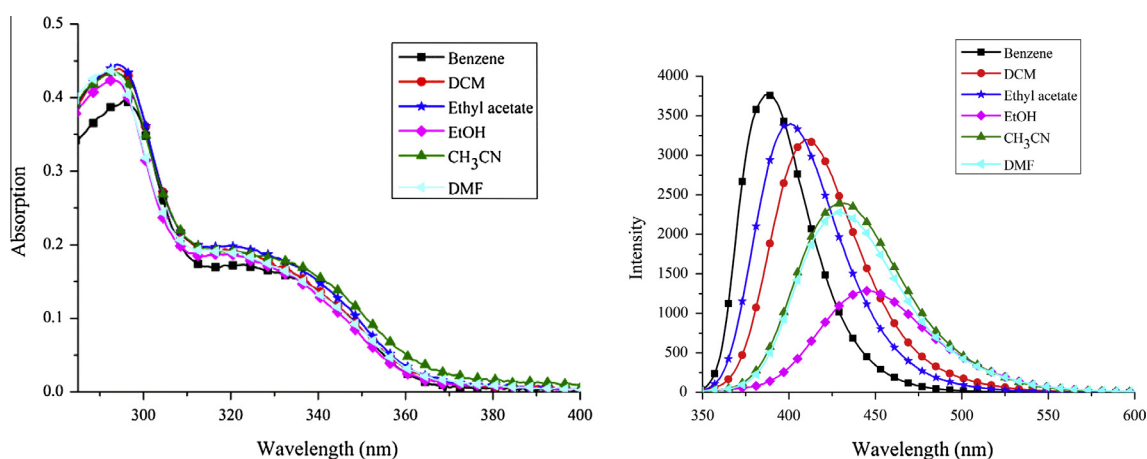


Fig. 2. Absorption spectra and One-Photon Excited Fluorescence (OPEF) of L in different solvents.

The fluorescence quantum yields (Φ)

The fluorescence quantum yields (Φ) were determined by using quinine sulfate as the reference according to the literature method [47]. Quantum yields were corrected as follows:

$$\Phi_s = \Phi_r \left(\frac{A_r \eta_s^2 D_s}{A_s \eta_r^2 D_r} \right)$$

where the s and r indices designate the sample and reference samples, respectively, A is the absorbance at λ_{exc} , η is the average refractive index of the appropriate solution, and D is the integrated area under the corrected emission spectrum.

Table 1 shows the quantum yields of L obtained in different solvents. The ethanol solvent show the least, which could be explained by the hydrogen bonds of ethanol molecules lowered some energy from the excited state of the molecules. However, the

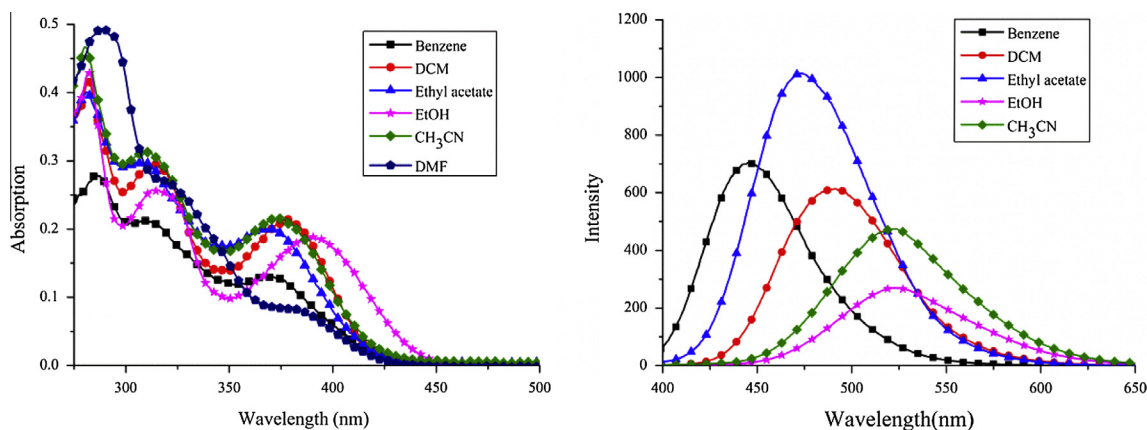


Fig. 3. Absorption spectra and One-Photon Excited Fluorescence (OPEF) of $ZnLCl_2$ in different solvents.

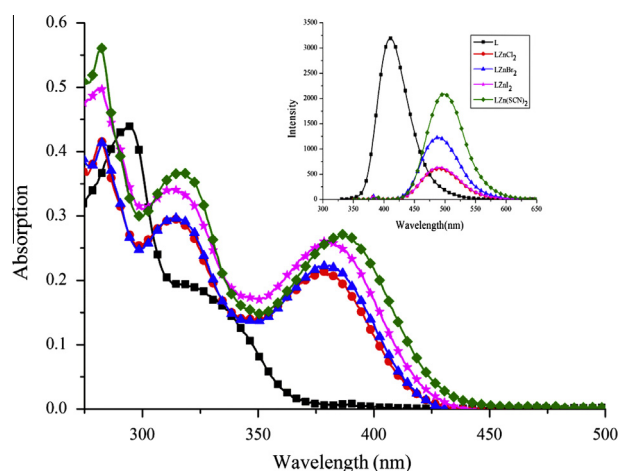


Fig. 4. Absorption spectra and One-Photon Excited Fluorescence (OPEF) of L, $ZnLCl_2$, $ZnLBr_2$, $ZnLl_2$, and $ZnL(SCN)_2$ in CH_2Cl_2 .

fluorescence quantum yields (Φ) show the decreasing tendency from the ligand to the corresponding complexes. It could be

explained that the strong spin–orbital coupling induced by mixing of the ligand (π and π^*) and metal d π orbital enhanced the nonradiative decay pathways.

Nonlinear optical properties

The NLO properties of $ZnLCl_2$ and $ZnLBr_2$ were measured by the Z-scan technique using a tunable femtosecond laser system. However, the other two complexes showed no response to NLO properties. Z-scan data for $ZnLCl_2$ and $ZnLBr_2$ in DMF at $1.0 \times 10^{-3} \text{ mol L}^{-1}$, were obtained under an open aperture and closed aperture configuration ($\lambda = 700 \text{ nm}$).

As shown in Fig. 5, the open-aperture transmittance was symmetric with respect to the focus ($z = 0$). The obvious minimum transmittance unambiguously indicated a biggish nonlinear absorption which was attributed to TPA effect. The two-photon absorption coefficient β and TPA cross-sections σ were determined by the open-aperture Z-scan technique. The theoretical data were fitted using the following equations [48,49]:

$$T(z, s = 1) = \sum_{m=0}^{\infty} \frac{[-q_0(Z)]^m}{(m+1)^{3/2}} \quad \text{for } |q_0| < 1 \quad (1)$$

$$q_0(Z) = \frac{\beta I_0 L_{\text{eff}}}{1 + \chi^2} \quad (2)$$

Table 2

Selected experimental and calculated optical data for the ligand and their Zinc(II) Complexes.

Compd.		OI ^a (Tc) ^b	ΔE (eV) ^c	Cal. λ_{max} (nm) ^d	Obs. λ_{max} (nm) ^e	f^f	Character ^g
L	1	H–2 → L+1(0.43)	4.25	292	295	0.2155	$\pi(\text{tpy}) \rightarrow \pi(\text{tpy})^*$
	2	H → L+1(0.52)	3.68	337	323	0.2662	$\pi(\text{cbz}) \rightarrow \pi(\text{tpy})^*$
$ZnLCl_2$	1	H–4 → L+4(0.43)	4.39	282	286	0.0377	$\pi(\text{cbz}) \rightarrow \pi(\text{tpy})^*$
	2	H–8 → L(0.51)	4.11	302	310	0.1280	$\pi \rightarrow \pi^*/\text{ICT}(\text{tpy} \rightarrow \text{tpy})$
	3	H–4 → L(0.68)	3.20	387	369	0.2768	$\text{ICT}/\pi \rightarrow \pi^*(\text{cbz} \rightarrow \text{tpy})$
$ZnLBr_2$	1	H–4 → L+4(0.50)	4.37	283	288	0.0637	$\pi(\text{cbz}) \rightarrow \pi(\text{tpy})^*$
	2	H–9 → L(0.60)	4.09	303	313	0.1748	$\pi \rightarrow \pi^*/\text{ICT}(\text{tpy} \rightarrow \text{tpy})$
	3	H–4 → L(0.50)	3.18	389	372	0.1556	$\text{ICT}/\pi \rightarrow \pi^*(\text{cbz} \rightarrow \text{tpy})$
$ZnLl_2$		H–5 → L+3(0.45)	4.36	284	286	0.0300	$\pi(\text{cbz}) \rightarrow \pi(\text{tpy})^*$
		H–9 → L(0.64)	4.09	303	315	0.2322	$\pi \rightarrow \pi^*/\text{ICT}(\text{tpy} \rightarrow \text{tpy})$
	3	H–5 → L(0.61)	3.15	394	374	0.1767	$\text{ICT}/\pi \rightarrow \pi^*(\text{cbz} \rightarrow \text{tpy})$
$ZnL(SCN)_2$	1	H–4 → L+3(0.57)	4.25	292	290	0.0828	$\pi(\text{cbz}) \rightarrow \pi(\text{tpy})^*$
	2	H–7 → L(0.63)	4.09	303	312	0.2152	$\pi \rightarrow \pi^*/\text{ICT}(\text{tpy} \rightarrow \text{tpy})$
	3	H–4 → L(0.69)	3.01	411	395	0.2508	$\text{ICT}/\pi \rightarrow \pi^*(\text{cbz} \rightarrow \text{tpy})$

^a Orbitals involved in the excitations.

^b Transition coefficients.

^c Excitation energies (eV).

^d Calculated peak position of the longest absorption band.

^e Observed peak position of the longest absorption band in benzene.

^f Oscillator Strengths.

^g tpy Instead of terpyridine; cbz instead of carbazole.

β was the nonlinear absorption coefficient of the solution, I_0 was the input intensity of laser beam at focus ($z = 0$) divided by $\pi\omega_0^2$, $L_{\text{eff}} = [1 - \exp(-\alpha_0 L)]/\alpha_0$ was the effective length with α_0 the linear absorption coefficient and L the sample length. $\chi = z/z_0$, $z_0 = \pi\omega_0^2/\lambda$ was the diffraction length of the beam with ω_0 the spot size at focus, λ was the wavelength of the beam and z was the sample position. So the nonlinear TPA coefficient β (in units of cm/GW) can be deduced. Furthermore, the σ could be determined by the following relationship [50]:

$$\sigma = h\gamma\beta/N_A d \times 10^{-3} \quad (3)$$

Here, h was the Planck constant, γ was the frequency of incident laser, σ was molecular TPA cross-section, N_A was the Avogadro number, and d was the concentration (in units of mol L⁻¹). Based on Eq. (3), the molecular TPA cross-section σ can be calculated.

By the equation of (2), the two-photon absorption coefficient β of ZnLCl₂ and ZnLBr₂ were 0.2783 cm/W and 0.1211 cm/W. As shown in Table 3, the two complexes exhibit two-photon absorptions with a maximum corresponding to $\sigma = 13,121$ and 5710 GM (Goepfert–Mayer units) at 700 nm. By close-aperture Z-scan, an effective third-order nonlinear optical refractive index g of the compounds can be derived from the equations: $\Delta T_{p-v} = 0.406(1-s)^{0.25}|\Delta\Phi_0|$, $\Delta\Phi_0 = \omega\gamma I_0 L_{\text{eff}}$, $\omega = 2\pi/\lambda$. In this experiment, $\Delta T_{p-v} = 0.1805$ and 0.1203, $s = 0.11$. Through the above formula, the refractive index γ of the compound were 4.75×10^{-17} m²/W and 3.15×10^{-17} m²/W. The effective third-order NLO susceptibility $\chi^{(3)}$ of the compound can be calculated according to the equations: $R_e c^{(3)} \text{esu} = 10^{-4} \epsilon_0 c^2 n_0^2 \gamma / \pi$, $I_m c^{(3)} \text{esu} = 10^{-2} \epsilon_0 c^2 n_0^2 \lambda \beta / 4\pi^2$,

$c^{(3)} = \{(R_e c^{(3)})^2 + (I_m c^{(3)})^2\}^{1/2}$, where ϵ_0 was the vacuum permittivity, c was the light velocity in vacuum, n_0 was the nonlinear refractive index of DMF ($n_0 = 1.43$), $\lambda = 700$ nm. The third-order nonlinear refractive index ($\chi^{(3)}$) was determined by the close-aperture Z-scan technique and the advantage of this method was that both the real and imaginary parts of $\chi^{(3)}$ can be determined simultaneously or consecutively. Calculated data were summarized in Table 3. From these data, it was obvious that both complexes possessed rather low imaginary part, which means minimal nonlinear optical losses. Also, the complexes with different coordination anions can influence their nonlinear optical properties.

The optical limiting property was a nonlinear optical process in which the transmittance of a material decreased as the input light intensity increases. The transmittance of pure DMF solvent in the same cell was also determined in order to eliminate the influences studied by a standard open-aperture Z-scan technique ($\lambda = 700$ nm) at the focus. Fig. S10 showed the transmitted energy changing with the increase of the incident beam intensity with a 1 mm cell of ZnLCl₂ in DMF at 1.0×10^{-3} mol L⁻¹. At low energy, the optical response obeyed Beer's law. When the input light energy reaches about 279 mW, the transmitted light energy started to deviate from normal linear behavior and exhibited a typical optical limiting effect. The damaging threshold was 640 mW, compared to that of C60 which was considered as an optical limiting materials [51]. These results certainly indicated that the ZnLCl₂ complex was valuable optical-limiting materials that should have great potential to excel in the advancement of practical devices.

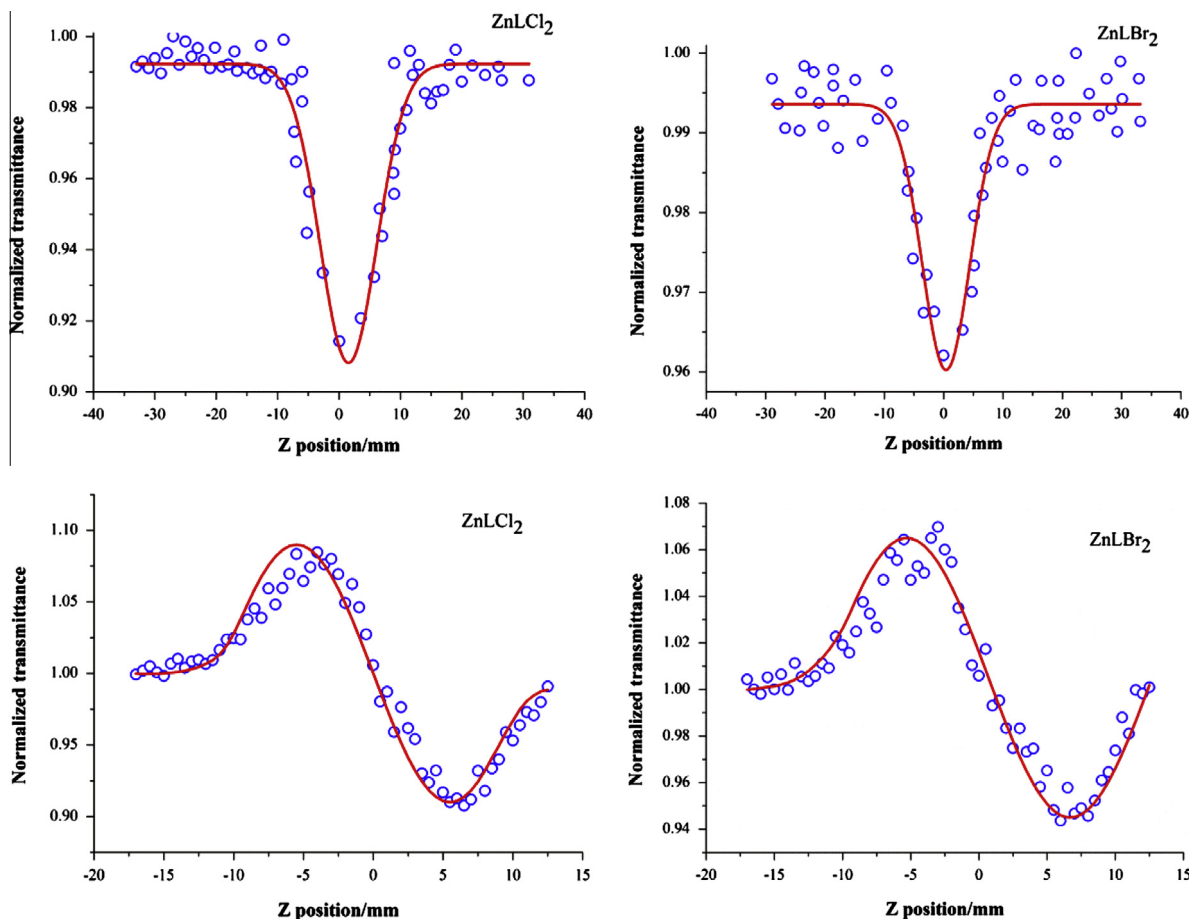


Fig. 5. Z-scan data for ZnLCl₂ and ZnLBr₂ in DMF at 1.0×10^{-3} mol L⁻¹, obtained under an open aperture and closed aperture configuration ($\lambda = 700$ nm). The blue dots are the experimental data and the solid curve is the theoretical fitting. (For interpretation of the references to colour in this figure legend, the reader is referred to the web version of this article.)

Table 3
Open and closed aperture Z-scan measurement data for the third-order nonlinearity parameters of ZnLCl₂ and ZnLBr₂.

Complex	ZnLCl ₂	ZnLBr ₂
Wavelength (nm)	700	700
γ (m ² /W)	4.75×10^{-17}	3.15×10^{-17}
$R_e(\chi^{(3)})$ (esu)	2.4561×10^{-15}	1.6246×10^{-15}
2PA coefficient β (cm/GW)	0.2783	0.1211
Two-photon cross section σ (GM)	13,121	5710
$I_m(\chi^{(3)})$ (esu)	8.0211×10^{-14}	3.4902×10^{-14}
$\chi^{(3)}$ (esu)	8.0248×10^{-14}	3.4940×10^{-14}

Conclusion

In conclusion, four novel Zn(II) terpyridine complexes (ZnLCl₂, ZnLBr₂, ZnLI₂, ZnL(SCN)₂) based on carbazole derivative with polyether group were designed, synthesized and fully characterized. The one photon photophysical properties were thoroughly investigated by means of colorimetric and fluorometric methods both experimentally and theoretically. The solvatochromism effect was significantly tested. A detailed investigation in the present study revealed that the different coordination anions can arouse largely different optical properties, which was confirmed by both experimentally and theoretically. The enhanced electron delocalized system can strengthen the fluorescence intensity and influence their quantum yields and fluorescent lifetime. Furthermore, the results of NLO determination revealed that two Zn(II) complexes possessed larger two-photon absorption cross-sections and ZnLCl₂ complex showed superior optical power limiting property which suggested a large polarizability, meeting the requirements for third-order NLO materials offering promise for applications in optical limiting in the near infrared region.

Acknowledgments

This work was supported by Grants from the National Natural Science Foundation of China (21271004, 51372003, 21271003 and 21275006), the Natural Science Foundation of Anhui Province (1208085MB22 and 1308085MB24), and Ministry of Education Funded Projects Focus on returned overseas scholar.

Appendix A. Supplementary material

Supplementary data associated with this article can be found, in the online version, at <http://dx.doi.org/10.1016/j.saa.2014.07.039>.

References

- [1] I. Eryazici, C.N. Moorefield, G.R. Newkome, *Chem. Rev.* 108 (2008) 1834–1895.
- [2] A. Winter, M.D. Hager, G.R. Newkome, *U.S. Schubert, Adv. Mater.* 23 (2011) 5728–5748.
- [3] U.S. Schubert, A. Winter, G.R. Newkome, *Terpyridine-Based Materials*, Wiley-VCH, Weinheim, 2011.
- [4] A. Wild, A. Winter, F. Schlütter, U.S. Schubert, *Chem. Soc. Rev.* 40 (2011) 1459–1511.
- [5] Ja.J. Concepcion, J.W. Jurss, M.K. Brennaman, P.G. Hoertz, A.O.T. Patrocínio, N.Y. Murakami Iha, J.L. Templeton, T.J. Meyer, *Acc. Chem. Res.* 42 (2009) 1954–1965.
- [6] M. Grätzel, *Acc. Chem. Res.* 42 (2009) 1788–1798.
- [7] J.A. Gareth Williams, *Chem. Soc. Rev.* 38 (2009) 1783–1801.
- [8] Y.H. Gao, J.Y. Wu, Y.M. Li, P.P. Sun, H.P. Zhou, J.X. Yang, S.Y. Zhang, B.K. Jin, Y.P. Tian, *J. Am. Chem. Soc.* 131 (2009) 5208–5213.
- [9] P. Wang, C.H. Leung, D.L. Ma, R.W.Y. Sun, S.C. Yan, Q.S. Chen, C.M. Che, *Angew. Chem. Int. Ed.* 50 (2011) 2554–2558.

- [10] R. Sakamoto, Y. Ohirabaru, R. Matsuoka, H. Maeda, S. Katagiri, H. Nishihara, *Chem. Commun.* 49 (2013) 7108–7110.
- [11] C. Truillet, F. Lux, J. Moreau, M. Four, L. Sancey, S. Chevreux, G. Boeuf, P. Perriat, C. Frochet, R. Antoine, P. Dugourd, C. Portefaix, C. Hoeffel, M. Barberi-Heyob, C. Terryn, L. van Gulick, G. Lemerrier, O. Tillement, *Dalton Trans.* 42 (2013) 12410–12420.
- [12] C.K. Prier, D.A. Rankic, D.W.C. MacMillan, *Chem. Rev.* 113 (7) (2013) 5322–5363.
- [13] Y. Yamanoi, J. Sendo, T. Kobayashi, H. Maeda, Y. Yabusaki, M. Miyachi, R. Sakamoto, H. Nishihara, *J. Am. Chem. Soc.* 134 (2012) 20433–20439.
- [14] O. Tutusaus, C.B. Ni, N.K. Szymczak, *J. Am. Chem. Soc.* 135 (2013) 3403–3406.
- [15] J.B. Gerken, M.L. Rigsby, R.E. Ruther, R.J. Pérez-Rodríguez, I.A. Guzei, R.J. Hamers, S.S. Stahl, *Inorg. Chem.* 52 (2013) 2796–2798.
- [16] A.V. Akimov, A.J. Neukirch, O.V. Prezhdo, *Chem. Rev.* 113 (2013) 4496–4565.
- [17] C.P. Zhang, H. Wang, A. Klein, C. Biewer, K. Stirnat, Y. Yamaguchi, L. Xu, V. Gomez-Benitez, D.A. Vicić, *J. Am. Chem. Soc.* 135 (2013) 8141–8144.
- [18] J.T. Hewitt, J.J. Concepcion, N.H. Damrauer, *J. Am. Chem. Soc.* 135 (2013) 12500–12503.
- [19] L. Wang, D.L. Ashford, D.W. Thompson, T.J. Meyer, J.M. Papanikolas, *J. Phys. Chem. C* 117 (2013) 24250–24258.
- [20] T. Sato, M. Higuchi, *Chem. Commun.* 49 (2013) 5256–5258.
- [21] P. Yang, M.S. Wang, J.J. Shen, M.X. Li, Zh.X. Wang, M. Shaob, X. He, *Dalton Trans.* 43 (2014) 1460–1470.
- [22] E.C. Constable, *Chem. Soc. Rev.* 36 (2007) 246–253.
- [23] J. Du, Z. Huang, X.Q. Yu, L. Pu, *Chem. Commun.* 49 (2013) 5399–5401.
- [24] C. Dragonetti, A. Colombo, M. Magni, P. Mussini, F. Nisic, D. Roberto, R. Ugo, A. Valore, A. Valsecchi, P. Salvadori, M.G. Lobello, F.D. Angelis, *Inorg. Chem.* 52 (2013) 10723–10725.
- [25] A. Wild, A. Winter, F. Schlütter, U.S. Schubert, *Chem. Soc. Rev.* 40 (2011) 1459–1511.
- [26] Q. Zhao, C. Huang, F.Y. Li, *Chem. Soc. Rev.* 40 (2011) 2508–2524.
- [27] C. Girardot, G. Lemerrier, J.C. Mulatier, J. Chauvin, P.L. Baldeck, C. Andraud, *Dalton Trans.* (2007) 3421–3426.
- [28] P. Shao, Y.J. Li, J. Yi, T.M. Pritchett, W.F. Sun, *Inorg. Chem.* 49 (2010) 4507–4517.
- [29] Z.Q. Ji, Y.J. Li, T.M. Pritchett, N.S. Makarov, J.E. Haley, Z.J. Li, M. Drobizhev, A. Rebane, W.F. Sun, *Chem. Eur. J.* 17 (2011) 2479–2491.
- [30] C. Yu, K.H.Y. Chan, K.M.C. Wong, V.W.W. Yam, *Chem. Eur. J.* 14 (2008) 4577–4584.
- [31] V.W.W. Yam, K.H.Y. Chan, K.M.C. Wong, N. Zhu, *Chem. Eur. J.* 11 (2005) 4535–4543.
- [32] K.M.C. Wong, W.S. Tang, X.X. Lu, N.Y. Zhu, V.W.W. Yam, *Inorg. Chem.* 44 (2005) 1492–1498.
- [33] S.C.F. Kui, Y.C. Law, G.S.M. Tong, W. Lu, M.Y. Yuen, C.M. Che, *Chem. Sci.* 2 (2011) 221–228.
- [34] P. Shao, Y.J. Li, W.F. Sun, *J. Phys. Chem. A* 112 (2008) 1172–1179.
- [35] M. Pawlicki, H.A. Collins, R.G. Denning, H.L. Anderson, *Angew. Chem. Int. Ed.* 48 (2009) 3244–3266.
- [36] Q. Zhang, Y.H. Gao, S.Y. Zhang, J.Y. Wu, H.P. Zhou, J.X. Yang, X.T. Tao, Y.P. Tian, *Dalton Trans.* 41 (2012) 7067–7072.
- [37] D. Ding, C.C. Goh, G.X. Feng, Z.J. Zhao, J. Liu, R.R. Liu, N. Tomczak, J.L. Geng, B.Z. Tang, L.G. Ng, B. Liu, *Adv. Mater.* 25 (2013) 6083–6088.
- [38] B. Xu, H.H. Fang, F.P. Chen, H.G. Lu, J. He, Y.W. Li, Q.D. Chen, H.B. Sun, W.J. Tian, *New J. Chem.* 33 (2009) 2457–2464.
- [39] J. Venturini, E. Koudoumas, S. Couris, J.M. Janot, P. Seta, C. Mathis, S. Leach, *J. Mater. Chem.* 12 (2002) 2071–2076.
- [40] R.R. Hu, J.W.Y. Lam, J.Z. Liu, H.H.Y. Sung, I.D. Williams, Z.N. Yue, K.S. Wong, M.M.F. Yuen, B.Z. Tang, *Polym. Chem.* 3 (2012) 1481–1489.
- [41] H. Woo, S. Cho, Y. Han, W.S. Chae, D.R. Ahn, Y.M. You, W. Nam, *J. Am. Chem. Soc.* 135 (2013) 4771–4787.
- [42] X.B. Xi, T.W. Dong, G. Li, Y. Cui, *Chem. Commun.* 47 (2011) 3831–3833.
- [43] S.M. Brombosz, A.J. Zucchero, R.L. Phillips, D. Vazquez, A. Wilson, U.H.F. Bunz, *Org. Lett.* 9 (2007) 4519–4522.
- [44] H.P. Zhou, F.X. Zhou, P. Wu, Z. Zheng, Z.P. Yu, Y.X. Chen, Y.L. Tu, L. Kong, J.Y. Wu, Y.P. Tian, *Dyes Pigm.* 91 (2011) 237–247.
- [45] Z. Zheng, Q. Zheng, Z.P. Yu, M.D. Yang, H.P. Zhou, J.Y. Wu, Y.P. Tian, *J. Mater. Chem. C* 1 (2013) 822–830.
- [46] L. Li, Y.P. Tian, J.X. Yang, P.P. Sun, J.Y. Wu, H.P. Zhou, S.Y. Zhang, B.K. Jin, X.J. Xing, C.K. Wang, M. Li, G.H. Cheng, H.H. Tang, W.H. Huang, X.T. Tao, M.H. Jiang, *Chem. Asian J.* 4 (2009) 668–680.
- [47] G.A. Crosby, J.N. Demas, *J. Phys. Chem.* 75 (1971) 991–1024.
- [48] M.S. Bahae, A.A. Said, T.H. Wei, D.J. Hagan, E.W.V. Stryland, *IEEE J. Quantum Electron.* 26 (1990) 760–769.
- [49] W. Zhao, P. Palittay-Muhoray, *Appl. Phys. Lett.* 65 (1994) 673–680.
- [50] K.K. Nagaraja, S. Pramodini, A. Santhosh Kumar, H.S. Nagaraja, P. Poornesh, D. Kekuda, *Opt. Mater.* 35 (2013) 431–439.
- [51] D.G. McLean, R.L. Sutherland, M.C. Brant, D.M. Brandelik, T. Pottenger, *Opt. Lett.* 18 (1993) 858–860.